journal of the mechanical behavior of biomedical materials 126 (2022) 104999

Contents lists available at ScienceDirect

Journal of the Mechanical Behavior of Biomedical Materials

journal homepage: www.elsevier.com/locate/jmbbm

A parameter reduced adaptive quasi-linear viscoelastic model for soft biological tissue in uniaxial tension

Othniel J. Aryeetey [a,b], Martin Frank [b], Andrea Lorenz [c], Sarah-Jane Estermann [a,b,c], Andreas G. Reisinger [a,b], Dieter H. Pahr [a,b,*]

[a] TU Wien, Institute of Lightweight Design and Structural Biomechanics, Gumpendorfer Straße 7, 1060, Vienna, Austria
[b] Karl Landsteiner University of Health Sciences, Department of Anatomy and Biomechanics, Division Biomechanics, Dr. Karl-Dorrek-Straße 30, 3500, Krems, Austria
[c] Austrian Center for Medical Innovation & Technology (ACMIT), Viktor Kaplan-Straße 2/1, 2700, Wiener Neustadt, Austria

ARTICLE INFO

Keywords:
Viscoelasticity
Quasi-linear
Parameter reduction
Soft tissue
Mechanical characterization

ABSTRACT

Mechanical characterisation of soft viscous materials is essential for many applications including aerospace industries, material models for surgical simulation, and tissue mimicking materials for anatomical models. Constitutive material models are, therefore, necessary to describe soft biological tissues in physiologically relevant strain ranges. Hereby, the adaptive quasi-linear viscoelastic (AQLV) model enables accurate modelling of the strain-dependent non-linear viscoelastic behaviour of soft tissues with a high flexibility. However, the higher flexibility produces a large number of model parameters.

In this study, porcine muscle and liver tissue samples were modelled in the framework of the originally published AQLV (3-layers of Maxwell elements) model using four incremental ramp-hold experiments in uniaxial tension. AQLV model parameters were reduced by decreasing model layers (*M*) as well as the number of experimental ramp-hold steps (*N*).

Leave One out cross validation tests show that the original AQLV model (3*M*4*N*) with 19 parameters, accurately describes porcine muscle tissue with an average R^2 of 0.90 and porcine liver tissue, R^2 of 0.86. Reducing the number of layers (*N*) in the model produced acceptable model fits for 1-layer (R^2 of 0.83) and 2-layer models (R^2 of 0.89) for porcine muscle tissue and 1-layer (R^2 of 0.84) and 2-layer model (R^2 of 0.85) for porcine liver tissue. Additionally, a 2 step (2*N*) ramp-hold experiment was performed on additional samples of porcine muscle tissue only to further reduce model parameters. Calibrated spring constant values for 2*N* ramp-hold tests parameters k_1 and k_2 had a 16.8% and 38.0% deviation from those calibrated for a 4 step (4*N*) ramp hold experiment. This enables further reduction of material parameters by means of step reduction, effectively reducing the number of parameters required to calibrate the AQLV model from 19 for a 3*M*4*N* model to 8 for a 2*M*2*N* model, with the added advantage of reducing the time per experiment by 50%.

This study proposes a 'reduced-parameter' AQLV model (2*M*2*N*) for the modelling of soft biological tissues at finite strain ranges. Sequentially, the comparison of model parameters of soft tissues is easier and the experimental burden is reduced.

1. Introduction

The mechanical characterisation of soft viscous materials is essential in applications such as in the aerospace and automotive industry for sound damping (Okeke et al., Greenrod), for anatomical models used in surgical training (Qiu et al., 2018; Barber et al., 2018; Randazzo et al., 2016) and for medical diagnosis of diseased tissue (Fovargue et al., 2018; Sinkus et al., 2018; Cao et al., 2017). However, this process can be difficult due to the non-linear, time-dependent behaviour of such materials, especially for soft biological tissue. Hence, complex material models with a large number of parameters are often required to model such material behaviour accurately.

The mechanical properties of different biological tissues vary over several orders of magnitude and are dependent on the strain level. For

* Corresponding author. TU Wien, Institute of Lightweight Design and Structural Biomechanics, Gumpendorfer Straße 7, 1060, Vienna, Austria.
E-mail address: dieter.pahr@kl.ac.at (D.H. Pahr).
URL: http://www.kl.ac.at (D.H. Pahr).

https://doi.org/10.1016/j.jmbbm.2021.104999
Received 2 September 2021; Received in revised form 4 November 2021; Accepted 24 November 2021
Available online 29 December 2021

example, the initial tensile elastic moduli of human adipose tissue is ≈ 3 kPa (Hammad et al., 2013), porcine hepatic tissue (Estermann et al., 2020a) at 14% strain ≈30 kPa, and for leporine skeletal muscle (Morrow et al., 2010) at 50% strain ≈450 kPa. Moreover, there is also a high variability of mechanical properties of a specific tissue of a single species due to age, gender or disease (MacManus et al., 2019). Hence, it is necessary that constitutive models effectively capture these material characteristics to enable differentiation and comparison across different soft biological tissues.

Previous literature on the constitutive modelling has shown that soft biological tissues exhibit a quasi-linear behaviour i.e. a linear stress-strain behaviour at low strains and a non-linear behaviour at higher strains (Liu and Bilston, 2000; Tan et al., 2013; Gao et al., 2010). Several constitutive models can be applied, whereby Fungs' quasi-linear viscoelastic (QLV) model is the most common one (Fung, 1993). The major advantage of the QLV model and

its extensions are twofold. Firstly, it is a non-linear viscoelastic model describing the mechanical behaviour of soft tissues very accurately. Secondly, it enables modelling of both the non-linear elastic and linear viscoelastic behaviour of soft tissue, with a single set of parameters. In contrast, other approaches implement a hyperelastic model to describe the non-linear elastic behaviour (Gao et al., 2010; Roan and Vemaganti, 2007; Veronda and Westmann, 1970; Umale et al., 2013), and a viscoelastic model to describe the viscous (relaxation or creep) response (Estermann et al., 2020b; Xu et al., 2020; Bu et al., 2019). In the QLV a single set of parameters, which may be 8 or less, depending on the specific adaptation used (Abramowitch and Woo, 2004; Jordan et al., 2009; Nava et al., 2008), is sufficient for modelling the material behaviour of soft biological tissues.

A limitation of the QLV model is, however, the assumption of a single reduced relaxation function at all strain levels. Simply put, if the QLV model is fitted to experimental stresses at a specific strain level it would not accurately predict stresses at different strain levels. To overcome this shortcoming, some extensions of the QLV model with a higher flexibility were proposed, such as that of Pipkin & Rogers (Pipkin and Rogers, 1968), the generalized Fung model by Pryse et al. (2003), the attenuated non-linear viscoelastic model (ANLV) proposed by Quaia et al. (2010) and the adaptive quasi-linear viscoelastic (AQLV) model proposed by Nekouzadeh et al. (2007). In general, the greater the flexibility of the model, the higher the number of parameters and computational expense required to fit the model to experimental data. Moreover, a large number of material parameters, makes comparison between various soft biological tissue as well as comparisons to polymeric tissue mimicking materials (TMMs), used in anatomical models, difficult and cumbersome. Hence, a trade-off between accurate modelling and fewer parameters would be advantageous.

The AQLV model is a non-linear viscoelastic model with a greater flexibility to model strain dependent behaviour but still simple to calibrate, compared to other models. Its parameters are calibrated by fitting model parameters to the stress responses of incremental ramp and hold experiments simultaneously. Further, the AQLV model is able to describe with a single set of parameters both the ramp loading response and the relaxation behaviour of soft biological tissue with good material fits (Nekouzadeh and Genin, 2013; Quaia et al., 2009a). The originally published model, however, produces a high number of model parameters (19) as it is modelled with 3 Maxwell (Mx) layers ($M = 3$) over 4 incremental ramp-hold tests ($N = 4$). Due to its flexibility, the number of layers and incremental ramp-hold phases can be reduced. As a result, the number of material parameters, as well as the experimental burden (time per single experiment), is also reduced.

Generally, previous studies aimed to increase the modeling accuracy and capability of constitutive models, thereby increasing the complexity of such models. In contrast, the aim of the current work is, to investigate the effect of a reduction in the AQLV model parameters on model accuracy and fitting. Here, uniaxial tensile experiments are carried out on a reasonable number of porcine skeletal muscle (M. longissimus) and porcine liver tissue (8 per group) to determine the non-linear viscoelastic response of these tissues based on the AQLV model. Further, the accuracy of a reduced form of the original AQLV model is investigated by sequentially reducing the model layers (M) and number of ramp-hold tests (N). This is the first time to the authors knowledge that the AQLV model would be applied to model porcine skeletal muscle and liver tissue and that a parameter reduction study is carried out on the AQLV model. The reduced model parameters will enable future finite element simulation of these tissues, ease the comparison of tested tissues and reduce the experimental burden associated with the calibration of a large number of tissue samples.

2. Methods

2.1. AQLV model theory

The AQLV model (originally described by Nekouzadeh et al. (Nekouzadeh et al., 2007; Nekouzadeh and Genin, 2013)) is a constitutive model that relates stress σ to strain ε via a simple multiplication between the viscoelastic strain $V^{(\varepsilon)}(t)$ and a pure non-linear function of strain $k(\varepsilon(t))$. $V^{(\varepsilon)}(t)$ incorporates the relaxation function $g(t)$, which describes the diminishing effect of the strain history on the current level of stress. The AQLV model can be interpreted as M Maxwell elements in parallel with a single spring (see Fig. 1A). In each layer i, $g_i(t)$ is chosen as a sum of exponential functions $g_i(t) = e^{-t/\tau_i}$ to represent the model in terms of parallel Maxwell elements, whereby the relaxation time τ_i is the ratio of the dashpot coefficient b_i to the spring constants k_i, $\tau_i = \frac{b_i}{k_i}$.

$$\sigma(t) = k(\varepsilon(t))V^{(\varepsilon)}(t) \tag{1}$$

$$V^{(\varepsilon)}(t) = \int_{-\infty}^{t} g(t-\tau)\frac{d\varepsilon(\tau)}{d\tau}d\tau \tag{2}$$

All the spring constants k_i and damper coefficients b_i are dependent on the overall tissue strain ε. For each Maxwell element i, a set of differential equations describes the stress and strain response:

$$\dot{V}_i + \frac{V_i}{\tau_i(\varepsilon)} = \dot{\varepsilon} \tag{3}$$

$$\sigma_i(t) = k_i(\varepsilon(t))\ V_i(t) \tag{4}$$

The relaxation times τ_i are therefore theoretically dependent on the overall tissue strain and not on the individual strains in each Maxwell element. A requirement of the model is that in each Maxwell element, both spring and damper elements should be proportional to the same non-linear function $\Psi_i(\varepsilon)$ of strain, since each element models a tissue-level strain-dependent relaxation mechanism. Hence the relaxation times τ_i are independent of strain:

$$\tau_i(\varepsilon) = \frac{b_i(\varepsilon)}{k_i(\varepsilon)} = \frac{b_i\Psi_i(\varepsilon)}{k_i\Psi_i(\varepsilon)} = \frac{b_i}{k_i} = \tau_i \tag{5}$$

Consequently, equations (3) and (4) become linear and their solution can be calculated in closed form from a linear convolution integral for a constant strain rate,

$$\dot{V}_i + \frac{V_i}{\tau_i(\varepsilon)} = \dot{\varepsilon} \rightarrow V_i(t) = \int_{-\infty}^{t} e^{-(t-\xi)/\tau_i}\frac{d\varepsilon(\xi)}{d\xi}d\xi \cdot i = 1, 2, \ldots M \tag{6}$$

where M is the total number of parallel Maxwell elements. The total stress can be given as the following summation:

$$\sigma(t) = \sigma_0(\varepsilon(t)) + \sum_{i=1}^{M} k_i(\varepsilon(t))\ V_i(t) \tag{7}$$

The residual stress $\sigma_0(\varepsilon(t))$ for the fully relaxed model is a pure function of strain and is related to the spring constant of the single spring

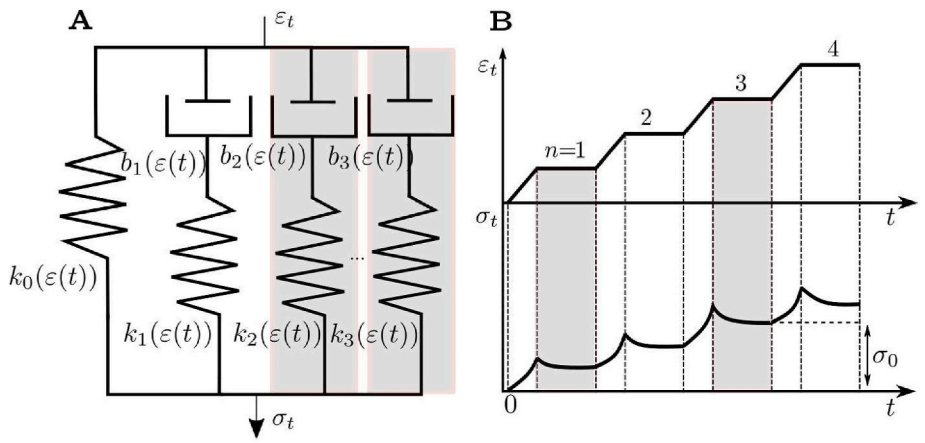

Fig. 1. A) Maxwell element representation of the original AQLV model (Nekouzadeh and Genin, 2013), showing the connection of non-linear springs k_i and dampers b_i. B) Strain-time inputs (top) and stress-time outputs (bottom) of a typical incremental ramp and hold experiment for the calibration of the original model with $N = 4$ levels. Highlighted (gray) are the elective Maxwell elements and ramp-hold steps that formulate the presented reduced models.

element $k_0(\varepsilon(t))$.

2.2. AQLV model calibration

The AQLV model is calibrated using an incremental ramp-hold protocol as seen in Fig. 1B. This involves equidistant ramp stretches $\Delta\varepsilon$ over stretch time.

T at a constant strain rate $\frac{\Delta\varepsilon}{T} = const$, followed by hold phases for sufficiently.

long times, with $\dot{\varepsilon} = 0$ to allow relaxation of the sample to an equilibrium stress σ_0. To obtain the stress-strain relation, a strain function for the nth ramp-hold test is given by:

$$\varepsilon_n(t) = \begin{cases} (n-1)\Delta\varepsilon, & t < 0 \\ (n-1)\Delta\varepsilon + \dfrac{\Delta\varepsilon}{T}t, & 0 < t < T \\ n\Delta\varepsilon, & t > T \end{cases} \tag{8}$$

and substituted into the equation for viscoelastic strain at each level $V_{i/n}^{(\varepsilon)}(t)$, ($i$th Maxwell layer, nth ramp-hold), represented for time phases between $0 < t < T$ given as:

$$V_{i/n}^{(\varepsilon)}(t) = \int_0^t g_i(t-\tau)\frac{\Delta\varepsilon}{T}d\tau = \frac{\Delta\varepsilon}{T}\gamma_i(t), \quad 0 < t < T \tag{9}$$

where by $\gamma_i(t)$ is the integral of $g_i(t)$. For each nth hold relaxation for time phases $t > T$, where T is the ramp time, the viscoelastic strain is given by:

$$V_{i/n}^{(\varepsilon)}(t) = \int_0^T g_i(t-\tau)\frac{\Delta\varepsilon}{T} = \frac{\Delta\varepsilon}{T}\left(\gamma_i(t) - \gamma_i(t-T)\right), \quad t > T \tag{10}$$

Incorporating equations (9) and (10) into equation (1) for the predicted stress $\sigma_{R/n}$ for ramp phases of the test gives:

$$\sigma_{R/n}(t) = \sigma_{0/n} + \frac{\Delta\varepsilon}{T}\sum_{i=1}^{M} k_{i/n}\gamma_i(t) \tag{11}$$

The predicted stress for the hold phase of each nth test is given by substituting equations (9) and (11) into equation (1):

$$\sigma_{H/n}(t) = \sigma_{0/n} + \frac{\Delta\varepsilon}{T}\sum_{i=1}^{M} k_{i/n}(\gamma_i(t) - \gamma_i(t-T)) \tag{12}$$

In the originally published model applied to neocartilage (Nekouzadeh and Genin, 2013), the number of calibration steps (N) used was 4 and the number of model layers i.e. parallel Maxwell elements M was 3.

The relaxation function represented as exponential shape functions can be given by:

$$g_1(t) = \tau_1\left(1 - e^{-t/\tau_1}\right),\ g_2(t) = \tau_2\left(1 - e^{-t/\tau_2}\right), \ldots$$

$$g_3(t) = \tau_3\left(1 - e^{-t/\tau_3}\right), \tag{13}$$

Substituting the shape functions into equation (11) gives the predicted hold phase stresses at each nth ramp-hold test as:

$$\sigma_{H/n}(t) = \sigma_{0/n} + \frac{\Delta\varepsilon}{T}\sum_{i=1}^{3} k_{i/n}\,\tau_i\left(e^{T/\tau_i} - 1\right)e^{-t/\tau_i} \tag{14}$$

Values for $\sigma_{0/n}$ and $k_{i/n}$ are obtained at each strain level (n). Values between obtained points are determined by means of a cubic spline interpolation as performed originally (Nekouzadeh and Genin, 2013). It is, however, possible to apply different interpolation functions such as a quadratic or exponential interpolation.

The values of τ_i and $k_{i/n}$ are calibrated using only the hold phase, whereby the integrals I_n are minimized, $\sigma_{H/n}(t)$ is the predicted hold stress, and $H_n(t)$

is the experimentally recorded relaxation stress:

$$I_n = \sum_n \int_T^{+\infty} \left(\frac{H_n(t) - \sigma_{H/n}(t)}{H_n(T)}\right)^2 dt \tag{15}$$

The fitted parameters are then implemented into equation (9) to predict ramp phase stresses. To account for non-linear strains in the ramp phase, experimentally obtained optical strains ($\varepsilon(t)$) might be implemented into the following adaptation of the equation (11):

$$\sigma(\varepsilon, t) = \sigma_0(\varepsilon(t)) + \frac{\Delta\varepsilon}{T}\sum_{i=1}^{3} k_i(\varepsilon(t))\tau_i e^{-t/\tau_i} \tag{16}$$

where k_i values have been implemented as a function, hence in the routine, $\sigma_0(\varepsilon(t))$ and $k_{i/n}(\varepsilon(t))$ are computed, in this case, from the cubic spline interpolation of $\sigma_{0/n}$, $k_{i/n}$ values, respectively.

2.3. Study design

In the present study, the mechanical response of eight samples each, of porcine skeletal muscle and porcine liver tissue at (large) strains was modelled. Calibration was performed with experimental data of only the hold relaxation stresses at different strain steps $N = 4$ with 3 Mx elements ($M = 3$) which describes the original (3-layer) model (see Fig. 1). The calibration was implemented numerically in Python 3 based on the original available code and validated against previous data from

Nekouzadeh et al. (Nekouzadeh and Genin, 2013) and Smith et al. (2010). Stresses in the ramp phase were then predicted using the obtained model parameters. The original Python functions were altered to implement parameter reduction techniques. To compare the quality of fit across the original and reduced models, the coefficient of determination (R^2) and the root mean square error (RMSE) were determined for each model (see section 2.4.3. for details). A leave one out cross validation (LOOCV) was performed for all samples to assess how well the model parameters of each AQLV model would predict future tissue samples. The process was performed for both porcine skeletal muscle and liver tissue.

2.4. Parameter reduction

2.4.1. Layer reduction

The originally published AQLV model (Nekouzadeh and Genin, 2013) uses 3 parallel Maxwell elements and is, hence, referred to as the 3-layer model. Calibration of soft tissue material parameters in the framework of the original AQLV model with $M = 3$ layers and using $N = 4$ strain levels (experimental ramp-hold levels) would involve identification of $M = 3$ relaxation times (τ_i), $N \cdot M$ spring constants $= 12$ and $N = 4$ equilibrium stresses (σ_0). The number of total material model parameters L follows from

$$L = M + N \cdot M + N \tag{17}$$

resulting in $L = 19$ material model parameters. Here, a 1- and 2-layer model ($M = 1$ and $M = 2$) and the usage of two or four strain levels (see Section 2.4.2) are further proposed. However, a decrease in accuracy of the model is expected with a reduction in the number of model parameters. The aim is to determine if reduced models could still reasonably model the viscoelastic behaviour of soft biological tissue similar to a AQLV model with three layers and four strain levels.

2.4.2. Reduction of strain levels

A further possibility of parameter reduction, as well as a means of reducing the experimental burden, is the reduction of the number of experimental steps (N) used for calibration (see Fig. 1B). Conventionally, four strain levels are used to interpolate the behaviour of the residual stress and spring constants between zero and the maximal experimental strain. Here, we propose the use of the calibrated values of the model parameters at two strain levels $N = 2$, instead of at all four strain levels ($N = 4$). Four additional muscle tissue samples were tested at 2 ramp-hold steps and k_1 and k_2 were obtained at those 2 strain levels (0.2 and 0.4 strain). A higher strain level was chosen to investigate how well the model predicts material behaviour close to the yield range of muscle tissue. However only values of k_1 and k_2 at 0.2 strain were compared to those obtained from a four ramp-hold ($N = 4$) experiment.

2.4.3. Average model parameters and fits

The material parameters ($\sigma_{0/n}, \tau_i, k_{i/n}$) of each model (3-,2-,1-layer) are obtained for each of the samples individually. The leave one out cross validation (LOOCV) is applied to the mean values of material parameters obtained.

The quality of model fits are compared using the coefficient of determination (R^2) and the root mean square error (RMSE). Hereby, R^2 and RMSE are determined for each tissue using the average of the 7 remaining tissue samples. Each R^2 and RMSE obtained from each individual prediction is measured and the mean of the values is reported. This describes how well a given set of material parameters would predict the next tissue sample.

2.4.4. Comparison to commonly used material properties

Although the AQLV model enables accurate modeling of soft biological tissue, it requires a large number of material parameters for calibration, which makes it cumbersome to compare. However, commonly used elastic and viscous parameters such as the instantaneous modulus (E_0, $\dot{\varepsilon} \to \infty$), long term modulus ($E_\infty$, $\dot{\varepsilon} \to 0$), storage modulus (E'), loss modulus (E'') and loss tangent ($tan\delta$) could be calculated based on the $k_{i/n}$ values at calibrated strain levels by the following equations, assuming linear visco-elasticity and small amplitude oscillations on top of an offset strain (Gutierrez-Lemini, 2014). It is however noted that these values only represent approximations to provide easier physical interpretation of AQLV model parameters and comparison to literature.

$$E'(\varepsilon(t)) = k_0(\varepsilon(t)) + \sum_{i=1}^{M} \frac{k_i(\varepsilon(t))\omega^2\tau_i^2}{1+\omega^2\tau_i^2} \tag{18}$$

$$E''(\varepsilon(t)) = \sum_{i=1}^{M} \frac{k_i(\varepsilon(t))\omega\tau_i}{1+\omega^2\tau_i^2} \tag{19}$$

where by the angular frequency (ω) is assumed to be 1 Hz throughout the current study, for 1 mm/s loading rate. The loss tangent ($\tan\delta$) is the ratio of the loss to storage modulus and is computed as:

$$\tan\delta\left(\varepsilon\left(t\right)\right) = \frac{E''(\varepsilon(t))}{E'(\varepsilon(t)} \tag{20}$$

Long term modulus (E_∞) and instantaneous modulus (E_0) are calculated as:

$$E_\infty(\varepsilon(t)) = \sigma_0(\varepsilon(t)) \tag{21}$$

$$E_0 = \sigma_0(\varepsilon(t)) + \sum_{i=1}^{M} k_i(\varepsilon(t)) \tag{22}$$

2.5. Sample preparation

Whole porcine skeletal muscle (M. logissimus) and liver organs were obtained fresh from a local abbattoir. Porcine skeletal muscle samples were directly sliced (see Fig. 2A), whilst Glisson's capsule of porcine liver tissue was firstly excised, leaving parenchyma tissue only (see Fig. 2B). Tissue was sliced into rectangular $75 \cdot 20 \cdot 5$ mm^3 ($L \cdot B \cdot T$) samples as described previously by Estermann et al. (2020b), for stress relaxation experiments. Specimens were stored in a physiological saline solution (9 g/l NaCl) at room temperature immediately after incision, until testing, to ensure hydration. A total of 12 porcine muscle (8 samples for 4N and 4 for 2N ramp-hold experiments) as well as 8 liver tissue specimens, were used for model calibration.

2.6. Mechanical testing

Experiments were performed with an electro-mechanical test machine

(ZwickiLine Z2.5, Zwick Roell GmbH, Ulm, Germany) in combination with a

100 N load cell (S2M HBM, Freiburg, Germany) and a data acquisition system

(QuantumX MX440B HBM, Freiburg, Germany) operated at 10 Hz (see Fig. 2C). A high-resolution camera (Sony α-6400, Sony, Tokyo, Japan) was used for optical video recording at 1 Hz.

Incremental ramp and hold experiments were performed to calibrate the AQLV model, as described previously by Nekouzadeh et al. (2007). Samples were preconditioned directly prior to experiments individually by clamping approximately 15 mm of one edge (top) and allowing to hang for a period of 300 s. In the meantime, white dot markers (GOM, Braunschweig, Germany) were placed slightly below the upper clamped region and above 15 mm from the bottom end to avoid bell ends and to ensure that the gauge area was vertical. These were used for strain tracking analysis with a point tracking algorithm described previously by Frank et al. (2018) (see Fig. 2A).

Effective gauge length was approximately 40 mm for both tissue types. Specimens were subsequently clamped on both edges. The tissues

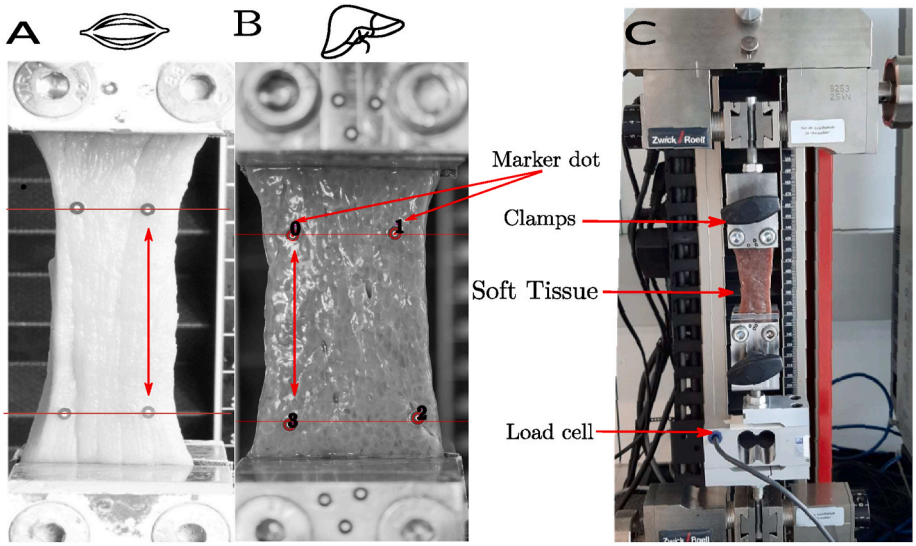

Fig. 2. A) Porcine muscle tissue and B) porcine liver tissue samples with markers used for optical strain tracking. Lines indicate the average position of markers on top and bottom of the sample. C) Mechanical test setup for uniaxial tensile testing, the sample is fixed with clamps and connected to a 100 N load cell mounted in an electro-mechanical testing machine.

were pulled at a speed of 0.1 mm/s, as performed in the original study by Nekouzadeh et al. (Nekouzadeh and Genin, 2013) for four equal strain steps ($N = 4$). The exact strains were determined optically with the strain tracking algorithm. The loading rates were assumed to be adequately small that inertial effects are negligible. The hold phases were 1500 s; this was tested prior to allow the tissue to reach an equilibrium state. Samples were hydrated intermittently by means of spraying to prevent severe dehydration in final stages of testing.

2.7. Stress and strain determination

Actual sample strains were obtained via digital image correlation (DIC). Hereby, the position of the markers is tracked over time and the relative displacement between the marker positions at the top and bottom is determined. Hence, engineering strain is computed as:

$$\varepsilon(t) = \frac{l(t) - l_0}{A_0} \tag{23}$$

where l_0 is the initial length (at zero-force) and $l(t)$ the actual length of the tissue. The uniaxial linear engineering stress (σ) is calculated from the axial measured force (f) and the cross-sectional area ($A_0 = B \cdot T$), measured with a caliper (prior to testing) and averaged at 3 positions, using the following equation:

$$\sigma(t) = \frac{f(t)}{A_0} \tag{24}$$

2.8. Statistical analysis

Model fits (R^2, RMSE) between each reduced model (1-, 2-layer) as well as results of step reduction for spring constant values k_1 and k_2 for step reduced models 2-layer models at 4 strain levels $2M4N$ and at 2 strain levels $2M2N$ were tested for statistical significance with respect to the 3-layer model using the Mann-Whitney U test for a significance level of $\alpha = 0.05$ implemented in Python 3.

3. Results

The mean experimentally determined stress curves with standard deviation for 8 porcine muscle tissue samples is shown in Fig. 3A and for 8 porcine liver tissue is shown in 3B. A relatively high variation in tissue stresses is still observed in both tissue types, with an increasing deviation in stresses at higher strain levels.

3.1. Comparison of AQLV models

Calibration of all model parameters was done for each sample individually for all samples to obtain material parameters ($\sigma_{0/n}$, $k_{i/n}$ and τ_i). R^2 and RMSE values from the Leave One Out cross validation (LOOCV) were calculated and tabulated for both porcine muscle and porcine liver tissue (see Table .1).

The mean parameters σ_0, $k_i(\varepsilon)$ were fitted with a cubic spline

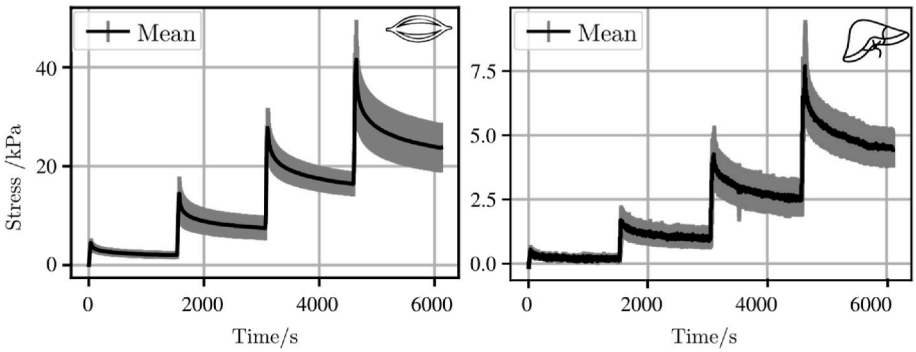

Fig. 3. Mean stress-time results of incremental ramp-hold tests (black) with standard deviation (gray) of A) porcine longissiumus muscle and B) porcine liver tissue.

Table 1
Mean ± standard deviations of time constants τ_i, residual stresses σ_0, spring constants k_i, for each strain level ε_n of AQLV models for porcine muscle and liver tissue.

Muscle	3-Layer				2-layer			1-layer	
	τ_1/s	τ_2/s	τ_3/s		τ_1/s	τ_2/s		τ_1/s	
	10 ± 7	88 ± 54	840 ± 442		25 ± 7	411 ± 44		130 ± 18	
ε_n	σ_0/kPa	k_1/kPa	k_2/kPa	k_3/kPa	σ_0/kPa	k_1/kPa	k_2/kPa	σ_0/kPa	k_1/kPa
0.06	2.0 ± 1.5	220 ± 100	22 ± 7.2	10 ± 2.7	2.0 ± 1.0	241 ± 74	22 ± 6.0	2.0 ± 0.9	164 ± 38
0.13	8.0 ± 4.8	650 ± 310	76 ± 44	41 ± 14	7.0 ± 3.1	720 ± 210	66 ± 20	8.0 ± 4.0	430 ± 100
0.20	13 ± 5.0	1020 ± 390	120 ± 34	69 ± 16	13 ± 5.3	1230 ± 400	120 ± 30	14 ± 2.8	790 ± 170
0.26	20 ± 6.3	1570 ± 790	180 ± 38	95 ± 22	18 ± 7.3	1510 ± 380	143 ± 46	20 ± 8.6	850 ± 230
Metric	$_R2$	RMSE/kPa			$_R2$	RMSE/kPa		$_R2$	RMSE/kPa
Mean	**0.90 ± 0.13**	**3.24 ± 1.74**			**0.89 ± 0.15**	**2.52 ± 1.6**		**0.83 ± 0.08**	**2.61 ± 2.54**
Liver	τ_1/s	τ_2/s	τ_3/s		τ_1/s	τ_2/s		τ_1/s	
	8.7 ± 4.7	88 ± 74	750 ± 320		18 ± 6.8	460 ± 82		168 ± 24	
ε_n	σ_0/kPa	k_1/kPa	k_2/kPa	k_3/kPa	σ_0/kPa	k_1/kPa	k_2/kPa	σ_0/kPa	k_1/kPa
0.04	0.1 ± 0.05	48 ± 28	13 ± 5.5	3.3 ± 2.2	0.1 ± 0.05	18 ± 10	4.4 ± 2.7	0.1 ± 0.06	6.7 ± 5.1
0.08	0.8 ± 0.3	120 ± 69	24 ± 9.4	8.4 ± 4.1	0.8 ± 0.3	87 ± 57	13 ± 8.3	0.8 ± 0.3	32 ± 22
0.12	2.5 ± 0.6	210 ± 61	56 ± 40	25 ± 11	2.4 ± 0.6	190 ± 31	30 ± 11	2.6 ± 0.8	100 ± 84
0.16	4.4 ± 1.1	470 ± 150	110 ± 100	45 ± 17	4.4 ± 1.1	330 ± 80	57 ± 31	4.3 ± 1.5	220 ± 22
Metric	$_R2$	RMSE/kPa			$_R2$	RMSE/kPa		$_R2$	RMSE/kPa
Mean	**0.86 ± 0.10**	**0.28 ± 0.06**			**0.85 ± 0.07**	**0.29 ± 0.22**		**0.84 ± 0.01**	**0.35 ± 0.15**

interpolation, to obtain intermediate points and are illustrated for porcine muscle tissue in Fig. 4.

A similar representative image was obtained for porcine liver tissue (see Appendix Figure 8). For the LOOCV, a single representative porcine muscle tissue sample was chosen to show the predictive behaviour of a 1-layer (blue), 2-layer (red) and 3-layer (black) AQLV model with respect to experimental (gray) data (see Fig. 5).

For porcine muscle tissue, it was observed, that the 3-layer and 2-layer model produced relatively close R^2 values (qualitative) fits, (0.90 ± 0.13 and 0.89 ± 0.15 respectively), whereas the 1-layer showed a worse fit (0.83 ± 0.08). Quantitatively, the 3-layer model, however showed a slightly higher RMSE (3.24 ± 1.74) kPa compared to the 2-layer (2.52 ± 1.61) kPa and 1-layer (2.61 ± 2.54) kPa model.

For porcine liver tissue, the 3-layer model showed better fits, albeit

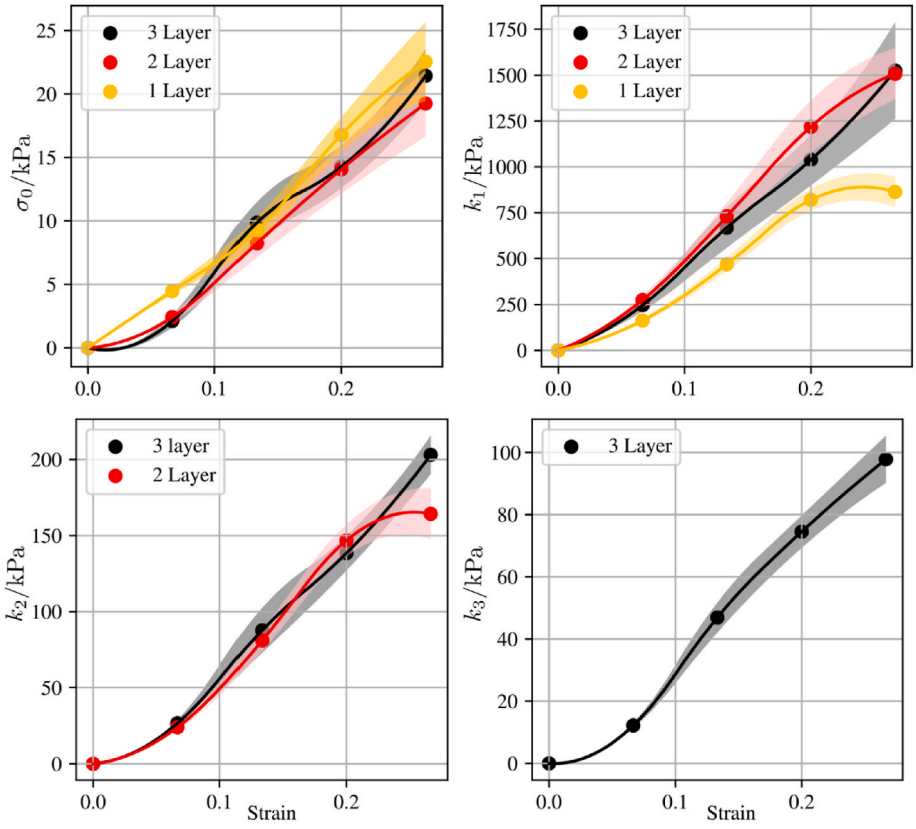

Fig. 4. Mean ± confidence interval equilibrium stresses (σ_0) and spring constants (k_i) values shown as a function of global strain (ε) of AQLV models of porcine muscle. Dots represent calibrated average values connected by cubic spline interpolations. Shadowed regions represent the 95% CI. A similar representative image was obtained for porcine liver tissue (see Appendix Figure 8).

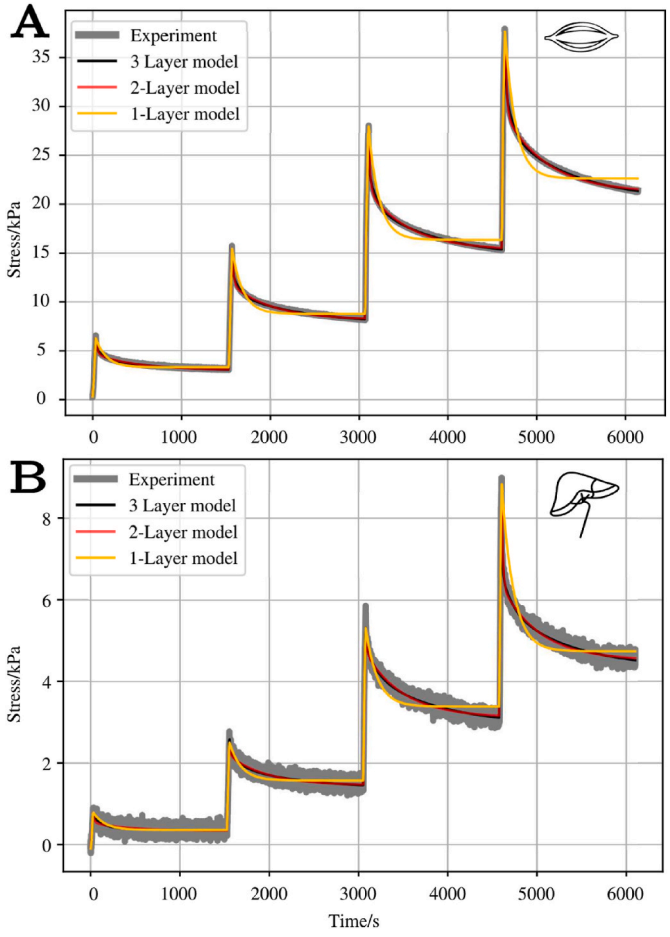

Fig. 5. Representative plot demonstrating the predictive behaviour of 1-layer (yellow), 2-layer (red) and 3-layer (black) AQLV models with respect to experimental (gray) data of a representative A) porcine muscle tissue and B) porcine liver tissue.

only slightly, both qualitatively (0.86 ± 0.10) and quantitatively (0.28 ± 0.06), as compared to the 2-layer (0.85 ± 0.07, 0.29 ± 0.22) and 1-layer (0.84 ± 0.01, 0.35 ± 0.15) AQLV models.

3.2. Reduction of strain levels

Four additional porcine muscle tissue samples were calibrated with a 2-layer AQLV model at a two-step incremental ramp-hold test performed on 4 porcine muscle samples. A representative muscle tissue sample calibrated at 2 ramphold steps ($N = 2$) is shown in Fig. 6 .

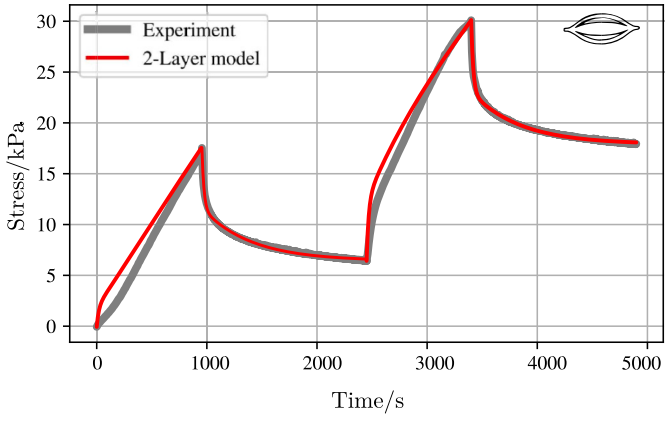

Fig. 6. Predictive behaviour of a 2-layer AQLV model (red) calibrated at 2 ramp and hold (2*N*) levels with respect to experimental data (gray).

Determined values of k_1 (1370 ± 310) kPa for a 2*M*2*N* AQLV model were

within the range of measured values for muscle tissue calibrated at 4 strain levels ($N = 4$) for a 3-layer AQLV model (1020 ± 390) kPa and 2-layer model (1230 ± 400) kPa calibrated at 4 ramp-hold steps ($N = 4$). There was no significant difference between the values of each pair of calibrated k_1 values ($p = 0.22$) based on the Mann-Whitney U test. This accounts for a maximum percentage deviation of ≈16.8% for k_1. Values determined for k_2 (76 ± 17) kPa for a 2*M*2*N* AQLV model showed a higher maximum percentage deviation (≈38%) as compared to k_2 determined 4 ramp hold steps for a 3-layer (120 ± 34) kPa and 2-layer (120 ± 30) kPa model. There was a significant difference for tests between each pair of calibrated k_2 values ($p = 0.006$) (see Fig. 7).

3.3. Comparison to commonly used material properties

To obtain material parameters that are commonly used in literature, the long term elastic modulus $E_\infty(\varepsilon(t))$, and instantaneous elastic modulus $E_0(\varepsilon(t))$ for each strain level was calculated from equations (21) and (22) respectively (see Table 2).

An increasing trend is observed with increasing strain level. While a decreasing stiffness is observed with decreasing model layers for both muscle tissue and liver tissue. The storage modulus E', loss modulus E'' and loss tangent $tan\delta$ per calibrated strain level n were also calculated (see Table 3), based on AQLV model parameters. Loss tangent values ranged from 0.073 to 0.086 for porcine muscle tissue and from 0.044 to 0.085 for porcine liver tissue with small variations with increasing strain level and model layer reduction.

4. Discussion

In this study, soft biological tissue (porcine muscle and liver), was modelled in the framework of the AQLV model under physiologically relevant large strains ($\varepsilon > 3\%$ (Wang et al., 2016)). Model parameter reduction was performed to ease comparison across different soft biological tissues and tissue mimicking materials, and further, to reduce the experimental burden.

Nie et al. (Nie et al., 1115) performed uniaxial tensile tests on porcine muscle and showed engineering stresses in the range of 25 kPa for 20% strain. Experimentally determined stresses for porcine muscle was ≈30 kPa for 20% strain obtained in the current study. Song et al. (2007) applied varying strain rates on porcine muscle tissue and showed similar stress ranges (< 100 kPa), to experimental stress values for applied strain of ≈40% on porcine muscle tissue (for a strain rate of 0.007/s). These differences in stresses can be related the influence of anatomical locations, of obtained tissue (Song et al., 2007) as well as differences in strain rates. Previously, porcine liver tissue was also tested in tension and compression with strains up to 20%, reporting stress levels in the range of 10 kPa by Chui et al. (2007). Similarly, in the current study, a stress amplitude of ≈8 kPa stress was determined for a strain level of 16%. These comparisons indicate a good overlap of our experimental stresses to previous literature.

Extraction of material properties from constitutive models is commonly performed by minimizing a target function, containing model stress and experimental stress with a set of material parameters. Results of modelling are usually compared by means of R^2 (Abramowitch and Woo, 2004; Wang et al., 2013; Zhang et al., 2008) or a root mean square error (RMSE) (Chui et al., 2007; Miller, 2000; Ramo et al., 2018; Troyer et al., 2012). R^2 values are a relative measure of fit and hence, are useful in comparing between models while RMSE values are absolute measures of fit and are useful for comparing models to experimental results. Thus, both measures were applied in this study.

Early literature on modelling of soft tissue was based on simple linear elastic models (Morrow et al., 2010; Van Sligtenhorst et al., 2006). Later,

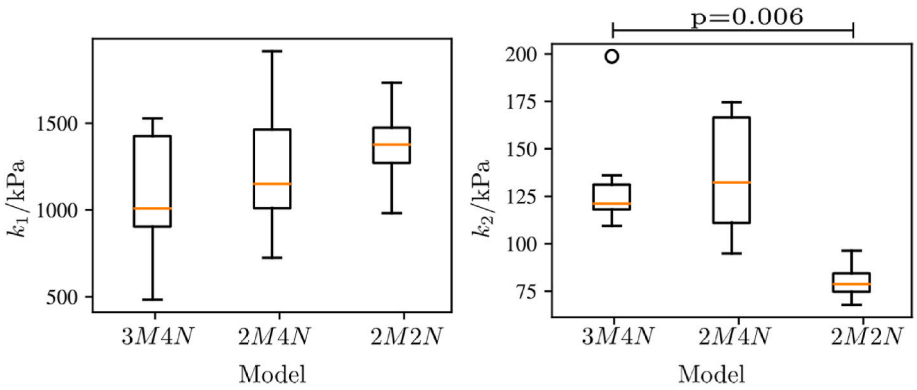

Fig. 7. Plots showing k_1 (left) and k_2 (right) calibrated with varying Maxwell layers M and ramp-holds N steps at 0.2 strain for porcine muscle tissue.

Table 2
Identified long term elastic modulus (E_∞) and instantaneous elastic modulus (E_0) based on identified spring constant values (k_i) for each strain level (n) for porcine muscle and liver tissue.

	3-layer		2-layer		1-layer	
ε	E_0	$E\infty$	E_0	$E\infty$	E_0	$E\infty$
Muscle						
0.06	2.0	250	2.0	270	2.0	170
0.13	7.5	650	7.0	720	7.7	440
0.20	13	1030	13	1240	14	68
0.26	20	1590	18	1530	20	870
Liver						
0.04	0.1	64	2.0	22	0.1	6.8
0.08	0.8	150	7.7	100	0.8	33
0.12	2.5	300	14	190	2.6	100
0.16	4.4	630	20	400	4.3	220

more complex hyperelastic material models were also used in modelling the non-linear behaviour observed in soft tissue such as in (Gao et al., 2010; Umale et al., 2013; Lu et al., 2014; Boubaker et al., 2006; Moerman et al., 2016). Chui et al. (2007) modelled liver tissue with a hyperelastic model and determined an RMSE in the range of 0.047 to 0.09 kPa. Miller et al. (Miller, 2000) applied a strain energy based non-linear hyper-viscoelastic model to describe monkey liver tissue with a single strain level up to 35%, reporting high model fits ($R^2 = 0.974$ to 0.996) for varying loading speeds. Loocke et al. (Van Loocke et al., 2006) measured strain dependent Young's moduli of porcine muscle tissue, modelled as transversely isotropic, at 30% strain with good experimental fits ($R^2 = 0.99$) and mean prediction errors of between 3.5% and 9.5%. Linear viscoelastic models such as the Prony series have also been applied to modelling soft biological tissue (Estermann et al., 2020a; Van Loocke et al., 2008; Wex et al., 2013), however, due to the complexity of soft tissue mechanical behaviour, non-linear viscoelastic models were further required (Best et al., 1994; Miller et al., 1997; Kemper et al., 2013). For example, Capilnasiu et al. (2020) applied viscoelastic adapted forms of the Mooney-Rivlin and Ogden exponential models to model liver tissue, while Loocke et al. (Van Loocke et al., 2009) modelled porcine muscle tissue in the framework of the QLV model at varying strain rates, and determined errors of $< 25\%$ between model and experimental data.

Generally, authors focused on the strain rate dependence of soft biological tissues at a single strain level; here however, the original AQLV model (3*M*4*N*) is applied to several strain levels, each tested at the same strain rate. Theoretically, the flexibility of the AQLV model should enable the variation of strain rates of a calibrated soft tissue, this however, requires further testing to be conclusive. In the current study, the AQLV model showed high model fits ($\approx$0.98) when samples are fitted individually, however slightly lower model fits ($R^2 = 0.90$ and $R^2 = 0.86$ for porcine muscle and liver respectively) were obtained when based on the LOOCV. The LOOCV shows how well the average set of parameters obtained from the set of specimens would predict a stress behaviour of a new tissue sample, these values were therefore lower due to the high variations in soft tissues. Previous studies also produced comparable individual model fits, for e.g. the QLV model for a single level ramp-hold test by Abramowitch et al. ($R^2 = 0.99$ (Abramowitch and Woo, 2004)) or a neo-Hookean based QLV model by MacManus et al. ($R^2 = 0.94$) (MacManus et al., 2019). Quaia et al., 2009a, 2009b, 2010 applied both the QLV and AQLV models to eye muscles in primates. They showed that the AQLV model provided a better fitting to experimental data but required a large number of parameters (35) as compared to the QLV model with (8) parameters and proposed a further extension of the models.

In this study, the AQLV model was applied as originally published and an investigation into material parameter reduction was conducted. A reduction of the number of model layers (M) as well as a reduction in the number of ramp-hold steps (N) for calibration of the AQLV model

Table 3
Identified storage modulus ($E^{'}$), loss modulus ($E^{''}$) and loss tangent (tanδ) per strain level based on identified spring stiffness values (k_i) for porcine muscle and liver tissue.

	3-layer			2-layer			1-layer		
ε	$E^{'}$	$E^{''}$	tanδ	$E^{'}$	$E^{''}$	tanδ	$E^{'}$	$E^{''}$	tanδ
Muscle									
0.06	254	19.0	0.074	300	24.4	0.081	164	14.2	0.086
0.13	758	56.7	0.074	783	62.6	0.079	434	37.2	0.085
0.20	1210	89.8	0.073	1360	107	0.079	790	68.0	0.085
0.26	1850	137	0.074	1660	132	0.079	860	73.6	0.085
Liver									
0.04	33.0	2.1	0.065	19.0	1.3	0.067	11.2	0.9	0.086
0.08	59.0	3.6	0.061	39.6	1.9	0.047	17.8	1.5	0.084
0.12	164	11.4	0.069	81.0	3.6	0.044	46.0	3.9	0.085
0.16	405	30.2	0.074	179	11.2	0.063	90.7	7.7	0.085

was performed. Model parameters are obtained by calibrating relaxation stresses with AQLV models. The non-linear elastic ramp fits are produced by implementing the calibrated parameters from hold equation Eqn. (12) into the ramp equation Eqn. (11), as originally described Nekouzadeh et al. (Nekouzadeh and Genin, 2013), which serves as a form of parameter validation. Alternatively, and for a possibly better fit, one could optimize the non-linear elastic response directly with the ramp stresses and obtain material parameters and response. The predictive ability of the original 3-layer (3*M*4*N*) model and 'reduced' (2*M*4*N*, 1*M*4*N*) models were also compared qualitatively based on the R^2 values. For porcine muscle tissue, there was no significant difference between the 3-layer (0.90 ± 0.13) and 2-layer model (0.89 ± 0.15) fits ($p = 0.47$). The 1-layer model showed notably poorer results (0.83 ± 0.08) however no significant difference with the original 3-layer AQLV model ($p = 0.16$) was determined. Similar results are observed for porcine liver tissue with no significant difference between the 3-layer (0.86 ± 0.10) and 2-layer (0.85 ± 0.08) model fits ($p = 0.44$). The 1-layer model also showed poorer results (0.84 ± 0.01) but was not significantly different from the 3-layer model ($p = 0.22$). The slight difference of only 1% when adding a third layer (in muscle and liver tissue) does not substantially add meaning to fits in terms of underlying internal processes. In contrast, subtle differences between tissues may still be highlighted with more relaxation time constants, but also may lead to ambiguity, as previously mentioned for a discrete QLV model (Babaei et al., 2015).

Quantitative results (RMSE) following LOOCV of porcine liver tissue indicated the original 3-layer model as the best fit model RMSE (0.284 ± 0.06) kPa as expected. The 2-layer model showed a RMSE (0.295 ± 0.219) kPa and the 1-layer model demonstrated a higher RMSE (0.346 ± 0.154) kPa. No significant difference between the 1-, and 2-layer models was observed ($p = 0.45$ and $p = 0.26$ respectively). For porcine muscle tissue the 1-layer and 2-layer models showed a relatively similar RMSE of (2.61 ± 2.54) kPa and (2.52 ± 1.61) kPa each better than the 3-layer model values. No significant difference however was observed between the results of the 1-layer and 2-layer models and the original 3-layer model ($p = 0.14$ and $p = 0.22$ respectively). An overall observed poorer performance of the 3-layer model at larger strains in the ramp phase was associated with the cubic spline interpolation, causing a greater oscillation of the model predicted stresses as compared to the experimental data. Hence, due to fewer parameters in the 1-layer model, the ramp prediction produces a better fit, compared to the 2-layer and 3-layer model. Since each phase (ramp and hold) are weighted equally, this offsets the poorer performance in the hold phase of the 1-layer model. The RMSE results are more conspicuous for porcine muscle tissue due to high stresses produced by porcine muscle tissue, as compared to liver tissue. A reasonable compromise in terms of accuracy and number of parameters was therefore the 2-layer AQLV model, with a total number of 14 parameters ($L = 14$).

The mean k_1 and k_2 for four samples of porcine muscle tissue tested at two strain levels (0.2 and 0.4 global strain) ($N = 2$) were determined for the 2-layer AQLV model. For k_1, which has the greatest effect on the predicted stresses, values of (1370 ± 310 kPa) were obtained for 2*M*2*N*, which were within a similar range of values calibrated at four strain levels ($N = 4$) for 2*M*4*N* (1230 ± 400) and 3*M*4*N* (1020 ± 390), given a maximum i.e greatest percentage deviation of 16.8%. There was no significant difference between values obtained k_1 values ($p = 0.22$). Values for k_2 were however slightly underestimated for ($N = 2$) (76 ± 17) kPa as compared to those obtained from ($N = 4$), 2*M*4*N* (120 ± 29) kPa and 3*M*4*N* (120 ± 34) kPa. There was a significant difference between values of k_2 obtained from a 4-step test and 2-step test ($p = 0.006$). This may lead to a slight underestimation in model stresses. Notwithstanding, the reduced AQLV model (2*M*2*N*) is able to accurately model the stress behaviour of a 2 ramp-hold experiment with high accuracy ($R^2 = 0.96 \pm 0.02$ and RMSE = 1.74

± 0.82) kPa. The proposed reduced-parameter AQLV model (2*M*2*N*) produces 8 parameters in total ($L = 8$). This would be a reasonable compromise between accuracy of the model, number of material parameters for comparison and experimental burden. Taken together, the AQLV model provides a comprehensive description of both, the non-linear elastic and viscoelastic behaviour of soft biological tissue; higher model fits are generally obtained for single strain level model calibrations, however these models are unable to accurately describe stress responses at varying strain levels as compared to the AQLV model. A higher accuracy is also possible with the AQLV model, however with at the expense of a high number of material parameters and greater experimental burden. It is noted that relaxation times often describe short and long-term responses of internal physical processes undergone during loading within the tissue. An example of such, would be the fast response of collagen fibres (≈7s–100s) as well as the long-term response of other constituent materials such as proteoglycans (Shen et al., 2011). However, it is difficult to specifically link these processes to parameters obtained from the AQLV models without testing individual tissue constituents.

To obtain commonly used material parameters, Nava et al. (2008) applied the QLV model to human hepatic tissue in vivo and obtained long term (E_∞) and instantaneous elastic modulus (E_0) to be 20 kPa and 60 kPa, respectively. Estermann et al. (2020a) estimated E_0 for porcine liver tissue to be around 130 ± 65 kPa. However, values for the elastic moduli of both porcine muscle and liver tissue in literature vary greatly due to variation of anatomical locations of tissues, test protocols, maximum strains, strain rates and whether or not optical strain measurement was used (Lu et al., 2014; Hollenstein et al., 2006; Chui et al., 2004). In the current study, values obtained from the AQLV model for E_0 for lower strains (4%–8%) are within the general range ($E_0 = 33$–58 kPa) of reported values. Interestingly, E_0 was observed to decrease with the number of Maxwell elements. Hence the response of reduced models to an instantaneous deformation is softer in comparison to the 3-layer model. This is unexpected, as an increase in the individual stiffness is expected in order to offset the loss of springs from the 3-layer model. These values are, however, based on the assumption of linear viscoelasticity of spring damper systems and are less useful for representing the true non-linear behaviour of soft tissue (Tschoegl and Tschoegl, 1989). It is also noted that the values obtained from the AQLV model, which represent the spring and dampers do not exist physically (Nekouzadeh et al., 2007), but are numerical values that enable modelling of material behaviour.

The loss tangent ($\tan\delta$) has been shown, in previous literature (Dunford et al., 2018; Zhang et al., 2017), to be a more robust material property and is more dependent on frequency or strain rate than on strain level. It has been reported in the range of 0.07–0.22 for porcine liver tissue (Estermann et al., 2020a; Wex et al., 2013). Similarly, results of approximations of loss tangents derived from current AQLV parameters (Table 3) show relatively small variations with across different strain levels. Loss tangent values for the 3-layer and 2-layer models were within a similar range (0.074 to 0.086) for porcine muscle, and in the range of (0.044 to 0.074) for porcine liver tissue. Higher values of loss tangent are observed for the 1-layer model. One could speculate that this may be due to the pronounced effect of the damper in the 'simpler' 1 layer model, however, this is conjecture without further analysis. These derived parameters are mostly only valid for small strain levels (linear viscoelasticity) are only useful for giving rough estimates to allow for the comparison of AQLV model parameters to existing literature.

In summary, the original AQLV model could accurately model the strain dependent non-linear viscoelastic behaviour of porcine muscle and liver tissue. The flexibility of the model enabled the proposal of a 'parameter-reduced' AQLV model, with a reduced number of parameters and a reduced experimental burden. This is especially advantageous for comparing several different biological tissues. Further, given the large variation in biological tissues due to age, sex and disease (Lund et al., 1999; Arroyave et al., 2015; Tsamis et al., 2013; Mazza et al., 2007), it is questionable if a much higher accuracy is advantageous over the decreased experimental burden and less than half of the material

parameters of the AQLV model. This becomes especially important when it is more important to gain both an accurate understanding of tissue behaviour as well as a representative order of magnitude of material properties.

5. Conclusion

This paper characterized the non-linear viscoelastic behaviour of soft biological tissue (porcine skeletal muscle and liver) at physiologically relevant large strains ($\varepsilon > 3\%$) based on the AQLV model. Adaptations of the originally published model were made to reduce the number of material parameters by reducing the number of layers i.e. the number of parallel spring damper systems in the standard AQLV model as well as the number of ramp-hold tests used for calibration. The adaptations eased the comparison of material parameters for the different soft biological tissues (porcine muscle and liver), while still providing sufficiently accurate modelling of their non-linear viscoelastic behaviour. In conclusion, a reduced AQLV model (2 Mx layers, 2 ramp-hold phases) is able to predict the visco-elastic behaviour of soft biological tissues with a sufficient accuracy. Hence, this proposed reduced AQLV model will ease comparison across different soft biological tissues in future and reduce the experimental burden associated with calibrating the model.

Credit author statement

Othniel J. Aryeetey: Methodology, Software, Validation, Formal analysis, Investigation, Visualisation, Writing-original draft. Martin Frank: Writing - review \& editing, Supervision. Andrea Lorenz: Conceptualization, Project administration, Funding acquisition. Sarah-Jane Estermann: Methodology, Resources. Andreas G. Reisinger: Conceptualization, Writing - review \& editing. Dieter H. Pahr: Conceptualization, Funding acquisition, Writing - review \& editing, Supervision.

Declaration of competing interest

The authors declare that they have no known competing financial interests or personal relationships that could have appeared to influence the work reported in this paper.

Acknowledgements

The research was a cooperation with the Austrian Center for Medical Innovation and Technology (ACMIT), funded in the “Forschung, Technologie & Innovation” (FTI) framework of the Provincial Government of Lower Austria (Land Niederoesterreich) under grant assignment number WST3-F2-528983/0052018. The authors want to appreciate the contribution of Lower Austria Landesgesundheitsagentur, legal entity of University Hospitals in Lower Austria, for providing the organizational framework to conduct this research. The authors acknowledge TU Wien Bibliothek for financial support through its Open Access Funding Programme.

Appendix A

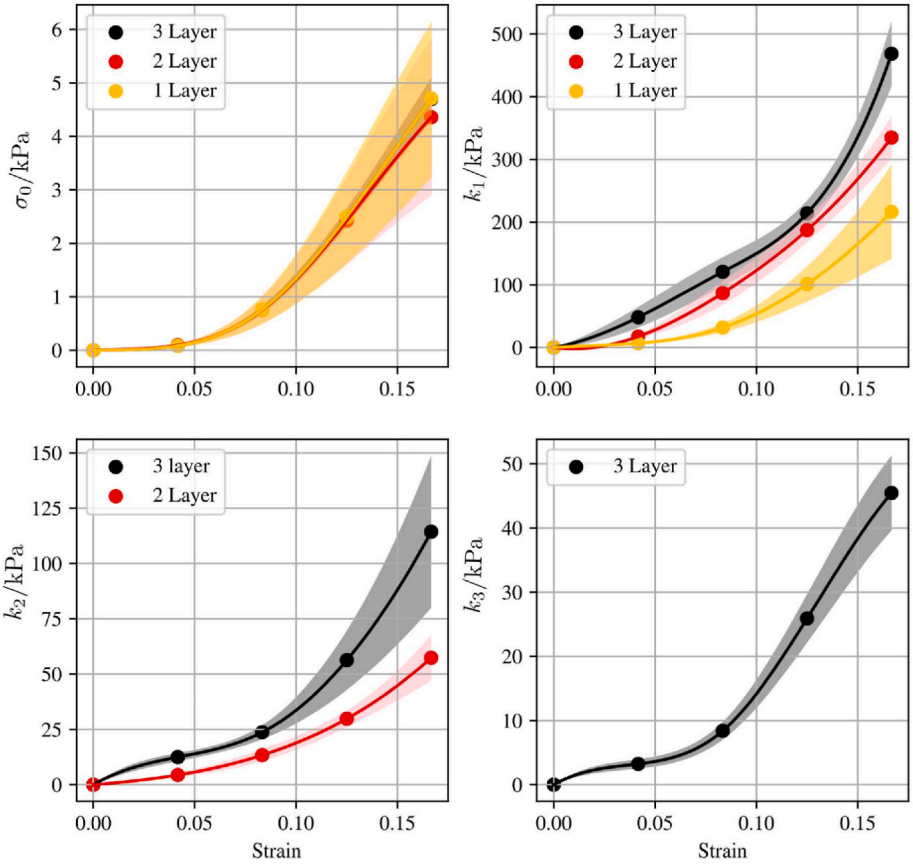

Fig. 8. Mean ± confidence interval of equilibrium stresses (σ_0) and spring constants (k_i) values of AQLV models of porcine liver. Dots represent calibrated average values connected by cubic spline interpolations. Shadowed regions represent the 95% CI.

References

Abramowitch, S.D., Woo, S.L., 2004. An improved method to analyze the stress relaxation of ligaments following a finite ramp time based on the quasilinear viscoelastic theory. J. Biomech. Eng. 126, 92–97.

Arroyave, G.A.I., Lima, R.G., Martins, P.A.L.S., Ramião, N., Jorge, R.M.N., 2015. Methodology for mechanical characterization of soft biological tissues: Arteries. Procedia Eng. 110, 74–81. https://www.sciencedirect.com/science/article/pii/S1877705815012539.

Babaei, B., Abramowitch, S.D., Elson, E.L., Thomopoulos, S., Genin, G.M., 2015. A discrete spectral analysis for determining quasi-linear viscoelastic properties of biological materials. J. R. Soc. Interface 12 (113), 20150707. https://doi.org/10.1098/rsif.2015.0707. https://doi.org/10.1098/rsif.2015.0707.

Barber, S.R., Jain, S., Son, Y.-J., Chang, E.H., 2018. Virtual functional endoscopic sinus surgery simulation with 3d-printed models for mixed-reality nasal endoscopy. Otolaryngol. Head Neck Surg. 159 (5), 933–937. https://doi.org/10.1177/0194599818797586. https://doi.org/10.1177/0194599818797586.

Best, T.M., McElhaney, J., Garrett, W.E., Myers, B.S., 1994. Characterization of the passive responses of live skeletal muscle using the quasi-linear theory of viscoelasticity. J. Biomech. 27 (4), 413–419. https://www.sciencedirect.com/science/article/pii/0021929094900175.

Boubaker, B., Pato, M., Pires, E., 2006. A finite element model of skeletal muscle. Virtual Phys. Prototyp. 1, 159–170.

Bu, Y., Li, L., Yang, C., Li, R., Wang, J., 2019. Measuring viscoelastic properties of living cells. Acta Mech. Solida Sin. 32 (5), 599–610. https://doi.org/10.1007/s10338-019-00113-7.

Cao, Y., Li, G.-Y., Zhang, X., Liu, Y.-L., 2017. Tissue-mimicking materials for elastography phantoms: a review. Extreme Mechanics Letters 17, 62–70. https://doi.org/10.1016/j.eml.2017.09.009. http://www.sciencedirect.com/science/article/pii/S2352431617301487.

Capilnasiu, A., Bilston, L., Sinkus, R., Nordsletten, D., 2020. Nonlinear viscoelastic constitutive model for bovine liver tissue. Biomech. Model. Mechanobiol. 1–22.

Chui, C., Kobayashi, E., Chen, X., Hisada, T., Sakuma, I., 2004. Combined compression and elongation experiments and non-linear modelling of liver tissue for surgical simulation. Med. Biol. Eng. Comput. 42 (6), 787–798. https://doi.org/10.1007/BF02345212.

Chui, C., Kobayashi, E., Chen, X., Hisada, T., Sakuma, I., 2007. Transversely isotropic properties of porcine liver tissue: experiments and constitutive modelling. Med. Biol. Eng. Comput. 45, 99–106.

Dunford, K.M., LeRoith, T., Kemper, A.R., 2018. Effects of postmortem time and storage fluid on the material properties of bovine liver parenchyma in tension. J. Mech. Behav. Biomed. Mater. 87, 240–255. https://www.sciencedirect.com/science/article/pii/S1751616118300511.

Estermann, S.-J., Pahr, D.H., Reisinger, A., 2020a. Hyperelastic and viscoelastic characterization of hepatic tissue under uniaxial tension in time and frequency domain. J. Mech. Behav. Biomed. Mater. 112, 104038. https://doi.org/10.1016/j.jmbbm.2020.104038. https://www.sciencedirect.com/science/article/pii/S1751616120305865.

Estermann, S.-J., Pahr, D.H., Reisinger, A., 2020b. Quantifying tactile properties of liver tissue, silicone elastomers, and a 3d printed polymer for manufacturing realistic organ models. J. Mech. Behav. Biomed. Mater. 104, 103630. https://doi.org/10.1016/j.jmbbm.2020.103630. http://www.sciencedirect.com/science/article/pii/S1751616119312949.

Fovargue, D., Kozerke, S., Sinkus, R., Nordsletten, D., 2018. Robust mr elastography stiffness quantification using a localized divergence free finite element reconstruction. Med. Image Anal. 44, 126–142. http://www.sciencedirect.com/science/article/pii/S1361841517301871.

Frank, M., Marx, D., Nedelkovski, V., Fischer, J.-T., Pahr, D.H., Thurner, P.J., 2018. Dehydration of individual bovine trabeculae causes transition from ductile to quasi-brittle failure mode. J. Mech. Behav. Biomed. Mater. 87, 296–305. https://www.sciencedirect.com/science/article/pii/S1751616118301462.

Fung, Y., 1993. Biomechanics: Mechanical Properties of Living Tissues. Springer.

Gao, Z., Lister, K., Desai, J.P., 2010. Constitutive modeling of liver tissue: experiment and theory. Ann. Biomed. Eng. 38 (2), 505–516. https://doi.org/10.1007/s10439-009-9812-0. https://doi.org/10.1007/s10439-009-9812-0.

Gutierrez-Lemini, D., 2014. Engineering Viscoelasticity, first ed. Springer, New York https://doi.org/10.1007/978-1-4614-8139-3.

Hammad, N., Mansfield, J., Green, E., Bell, J., Knight, B., Liversedge, N., Tham, J.C., Welbourn, R., Shore, A., Kos, K., Winlove, C., 2013. The mechanical properties of human adipose tissues and their relationships to the structure and composition of the extracellular matrix. Am. J. Physiol. Endocrinol. Metabol. 305 https://doi.org/10.1152/ajpendo.00111.

Hollenstein, M., Nava, A., Valtorta, D., Snedeker, J.G., Mazza, E., 2006. Mechanical characterization of the liver capsule and parenchyma. In: Harders, M., Székely, G. (Eds.), Biomedical Simulation. Springer Berlin Heidelberg, Berlin, Heidelberg, pp. 150–158.

Jordan, P., Socrate, S., Zickler, T.E., Howe, R.D., 2009. Papers from the Second International Conference on the Mechanics of Biomaterials and Tissues. Constitutive Modeling of Porcine Liver in Indentation Using 3d Ultrasound Imaging, vol. 2, pp. 192–201, 2. http://www.sciencedirect.com/science/article/pii/S1751616108000726.

Kemper, A.R., Santago, A.C., Stitzel, J.D., Sparks, J.L., Duma, S.M., 2013. Effect of strain rate on the material properties of human liver parenchyma in unconfined compression. J. Biomech. Eng. 135 (10), 104503. https://doi.org/10.1115/1.4024821. https://app.dimensions.ai/details/publication/pub.1062150139.

Liu, Z., Bilston, L., 2000. On the viscoelastic character of liver tissue: experiments and modelling of the linear behaviour. Biorheology 37, 191–201.

Lu, Y.-C., Kemper, A.R., Untaroiu, C.D., 2014. Effect of storage on tensile material properties of bovine liver. J. Mech. Behav. Biomed. Mater. 29, 339–349. https://www.sciencedirect.com/science/article/pii/S1751616113003238.

Lund, O., Chandrasekaran, V., Grocott-Mason, R., Elwidaa, H., Mazhar, R., Khaghani, A., Mitchell, A., Ilsley, C., Yacoub, M.H., 1999. Primary aortic valve replacement with allografts over twenty-five years: valve-related and procedure-related determinants of outcome. J. Thorac. Cardiovasc. Surg. 117, 77–90 discussion 90–1.

MacManus, D.B., Maillet, M., O'Gorman, S., Pierrat, B., Murphy, J.G., Gilchrist, M.D., 2019. Sex- and age-specific mechanical properties of liver tissue under dynamic loading conditions. J. Mech. Behav. Biomed. Mater. 99, 240–246. https://www.sciencedirect.com/science/article/pii/S1751616119303091.

Mazza, E., Nava, A., Hahnloser, D., Jochum, W., Bajka, M., 2007. The mechanical response of human liver and its relation to histology: an in vivo study. Med. Image Anal. 11 (6), 663–672. https://www.sciencedirect.com/science/article/pii/S1361841507000667.

Miller, K., 2000. Constitutive modelling of abdominal organs. J. Biomech. 33, 367–373.

Miller, C.E., Vanni, M.A., Keller, B.B., 1997. Characterization of passive embryonic myocardium by quasi-linear viscoelasticity theory. J. Biomech. 30 (9), 985–988. https://doi.org/10.1016/S0021-9290(97)00048-1. http://www.sciencedirect.com/science/article/pii/S0021929097000481.

Moerman, K.M., Simms, C.K., Nagel, T., 2016. Control of tension-compression asymmetry in ogden hyperelasticity with application to soft tissue modelling. J. Mech. Behav. Biomed. Mater. 56, 218–228. https://www.sciencedirect.com/science/article/pii/S1751616115004452.

Morrow, D.A., Haut Donahue, T.L., Odegard, G.M., Kaufman, K.R., 2010. Transversely isotropic tensile material properties of skeletal muscle tissue. J. Mech. Behav. Biomed. Mater. 3 (1), 124–129. https://www.sciencedirect.com/science/article/pii/S1751616109000472.

Nava, A., Mazza, E., Furrer, M., Villiger, P., Reinhart, W.H., 2008. In vivo mechanical characterization of human liver. Med. Image Anal. 12 (2), 203–216. https://www.sciencedirect.com/science/article/pii/S1361841507001004.

Nekouzadeh, A., Genin, G.M., 2013. Adaptive Quasi-Linear Viscoelastic Modeling. Ch. 1. Springer Berlin Heidelberg, Berlin, Heidelberg, pp. 47–83. https://doi.org/10.1007/8415_2012_142. https://doi.org/10.1007/8415_2012_142.

Nekouzadeh, A., Pryse, K., Elson, E., Genin, G., 2007. A simplified approach to quasi-linear viscoelastic modeling. J. Biomech. 40, 3070–3078. https://doi.org/10.1016/j.jbiomech.2007.03.019.

X. Nie, J.-I. Cheng, W. W. Chen, T. Weerasooriya, Dynamic tensile response of porcine muscle, J. Appl. Mech. 78 (2). doi: 10.1115/1.4002580.

C. Okeke, A. Thite, J. Durodola, N. Fellows, M. Greenrod, Modelling of hyperelastic polymers for automotive lamps under random vibration loading with proportional damping for robust fatigue analysis, Procedia Structural Integrity 13.

Pipkin, A., Rogers, T., 1968. A non-linear integral representation for viscoelastic behaviour. J. Mech. Phys. Solid. 16 (1), 59–72.

Pryse, K.M., Nekouzadeh, A., Genin, G.M., Elson, E.L., Zahalak, G.I., 2003. Incremental mechanics of collagen gels: new experiments and a new viscoelastic model. Ann. Biomed. Eng. 31, 1287–1296.

Qiu, K., Haghiashtiani, G., McAlpine, M.C., 2018. 3d printed organ models for surgical applications. Annu. Rev. Anal. Chem. 11 (1), 287–306. https://doi.org/10.1146/annurev-anchem-061417-125935 pMID: 29589961. arXiv: https://doi.org/10.1146/annurev-anchem-061417-125935. doi:10. 1146/annurev-anchem-061417-125935.

Quaia, C., Ying, H.S., Optican, L.M., 2009a. The viscoelastic properties of passive eye muscle in primates. ii: testing the quasi-linear theory. PLoS One 4 e6480–e6480. https://www.ncbi.nlm.nih.gov/pmc/articles/PMC2715107/, 19649257.

Quaia, C., Ying, H.S., Nichols, A.M., Optican, L.M., 2009b. The viscoelastic properties of passive eye muscle in primates. i: static forces and step responses. PLoS One 4 (4), e4850. https://doi.org/10.1371/journal.pone.0004850. https://doi.org/10.1371/journal.pone.0004850.

Quaia, C., Ying, H.S., Optican, L.M., 2010. The viscoelastic properties of passive eye muscle in primates. iii: force elicited by natural elongations. PLoS One 5 (3), e9595. https://doi.org/10.1371/journal.pone.0009595. https://doi.org/10.1371/journal.pone.0009595.

Ramo, N.L., Puttlitz, C.M., Troyer, K.L., 2018. The development and validation of a numerical integration method for non-linear viscoelastic modeling. PLoS One 13 e0190137–e0190137. https://www.ncbi.nlm.nih.gov/pmc/articles/PMC5749772/, 29293558.

Randazzo, M., Pisapia, J.M., Singh, N., Thawani, J.P., 2016. 3d printing in neurosurgery: a systematic review. Surg. Neurol. Int. 7 (33), S801–S809. https://doi.org/10.4103/2152-7806.194059. https://doi.org/10.4103/2152-7806.194059.

Roan, E., Vemaganti, K., 2007. The nonlinear material properties of liver tissue determined from no-slip uniaxial compression experiments. J. Biomech. Eng. 129, 450–456.

Shen, Z.L., Kahn, H., Ballarini, R., Eppell, S.J., 2011. Viscoelastic properties of isolated collagen fibrils. Biophys. J. 100, 3008–3015. https://www.ncbi.nlm.nih.gov/pmc/articles/PMC3123930/, 21689535.

Sinkus, R., Lambert, S., Abd-Elmoniem, K.Z., Morse, C., Heller, T., Guenthner, C., Ghanem, A.M., Holm, S., Gharib, A.M., 2018. Rheological determinants for simultaneous staging of hepatic fibrosis and inflammation in patients with chronic liver disease. NMR Biomed. 31 (10), e3956 https://doi.org/10.1002/nbm.3956. https://doi.org/10.1002/nbm.3956.

smith, d., komaragiri, u., tanov, r. Smith, D., Komaragiri, U., Tanov, R., 2010. Calibration of Nonlinear Viscoelastic Materials in Abaqus Using the Adaptive Quasi-Linear Viscoelastic Model. Similia Customer Conference.

Song, B., Chen, W., Ge, Y., Weerasooriya, T., 2007. Dynamic and quasi-static compressive response of porcine muscle. J. Biomech. 40 (13), 2999–3005. https://www.sciencedirect.com/science/article/pii/S0021929007000693.

Tan, K., Cheng, S., Jug'e, L., Bilston, L.E., 2013. Characterising soft tissues under large amplitude oscillatory shear and combined loading. J. Biomech. 46 (6), 1060–1066. http://www.sciencedirect.com/science/article/pii/S0021929013000717.

Troyer, K.L., Estep, D.J., Puttlitz, C.M., 2012. Viscoelastic effects during loading play an integral role in soft tissue mechanics. Acta Biomater. 8 (1), 234–243. https://doi.org/10.1016/j.actbio.2011. 07.035. http://www.sciencedirect.com/science/article/pii/S1742706111003448.

Tsamis, A., Krawiec, J.T., Vorp, D.A., 2013. Elastin and collagen fibre microstructure of the human aorta in ageing and disease: a review. J. R. Soc. Interface 10, 20121004.

Tschoegl, N.W., Tschoegl, N.W., 1989. Energy storage and dissipation in a linear viscoelastic material. In: The Phenomenological Theory of Linear Viscoelastic Behavior: an Introduction. Springer Berlin Heidelberg, Berlin, Heidelberg, pp. 443–488. https://doi.org/10.1007/978-3-642-73602-5_9.

Umale, S., Deck, C., Bourdet, N., Dhumane, P., Soler, L., Marescaux, J., Willinger, R., 2013. Experimental mechanical characterization of abdominal organs: liver, kidney & spleen. J. Mech. Behav. Biomed. Mater. 17, 22–33. https://www.sciencedirect.com/science/article/pii/S1751616112002056.

Van Loocke, M., Lyons, C.G., Simms, C.K., 2006. A validated model of passive muscle in compression. J. Biomech. 39, 2999–3009.

Van Loocke, M., Lyons, C.G., Simms, C.K., 2008. Viscoelastic properties of passive skeletal muscle in compression: stress-relaxation behaviour and constitutive modelling. J. Biomech. 41, 1555–1566.

Van Loocke, M., Simms, C.K., Lyons, C.G., 2009. Viscoelastic properties of passive skeletal muscle in compression-cyclic behaviour. J. Biomech. 42, 1038–1048.

Van Sligtenhorst, C., Cronin, D.S., Wayne Brodland, G., 2006. High strain rate compressive properties of bovine muscle tissue determined using a split hopkinson bar apparatus. J. Biomech. 39, 1852–1858.

Veronda, D., Westmann, R., 1970. Mechanical characterization of skin—finite deformations. J. Biomech. 3 (1), 111–124. https://doi.org/10.1016/0021-9290(70)90055-2. https://www.sciencedirect.com/science/article/pii/0021929070900552.

Wang, X., Schoen, J., Rentschler, M., 2013. A quantitative comparison of soft tissue compressive viscoelastic model accuracy. J. Mech. Behav. Biomed. Mater. 20C, 126–136.

Wang, K., Wu, C., Qian, Z., Zhang, C., Wang, B., Vannan, M.A., 2016. Dual- material 3d printed metamaterials with tunable mechanical properties for patient-specific tissue-mimicking phantoms. Additive Manufacturing 12, 31–37. https://doi.org/10.1016/j.addma.2016.06.006. http://www.sciencedirect.com/science/article/pii/S221486041630118X.

Wex, C., Stoll, A., Fröhlich, M., Arndt, S., Lippert, H., 2013. How preservation time changes the linear viscoelastic properties of porcine liver. Biorheology 50 (3–4), 115–131.

Xu, Q., Engquist, B., Solaimanian, M., Yan, K., 2020. A new nonlinear viscoelastic model and mathematical solution of solids for improving prediction accuracy. Sci. Rep. 10 (1), 2202. https://doi.org/10.1038/s41598-020-58240-y.

Zhang, M., Nigwekar, P., Castaneda, B., Hoyt, K., Joseph, J.V., di Sant'Agnese, A., Messing, E.M., Strang, J.G., Rubens, D.J., Parker, K.J., 2008. Quantitative characterization of viscoelastic properties of human prostate correlated with histology. Ultrasound Med. Biol. 34 (7), 1033–1042. https://doi.org/10.1016/j.ultrasmedbio.2007.11.024. https://doi.org/10.1016/j.ultrasmedbio.2007.11.024.

Zhang, X., Gao, X., Zhang, P., Guo, Y., Lin, H., Diao, X., Liu, Y., Dong, C., Hu, Y., Chen, S., Chen, X., 2017. Dynamic mechanical analysis to assess vis- coelasticity of liver tissue in a rat model of nonalcoholic fatty liver disease. Med. Eng. Phys. 44, 79–86. https://www.sciencedirect.com/science/article/pii/S1350453317300668.